Journal of Colloid and Interface Science **252,** 102–108 (2002)
doi:10.1006/jcis.2002.8459

Stability of Dispersions of Colloidal Hematite/Yttrium Oxide Core-Shell Particles

R. C. Plaza, A. Quirantes, and A. V. Delgado[1]

Department of Applied Physics, Faculty of Sciences, University of Granada, 18071 Granada, Spain

Received February 11, 2002; accepted April 30, 2002; published online July 2, 2002

The colloidal stability of suspensions of hematite/yttria core/shell particles is investigated in this work and compared with that of the pure hematite cores. The different electrical surface characteristics of yttrium and iron oxides, as well as the diameters of both types of spherical particles, dominate the overall process of particle aggregation. The aggregation kinetics of the suspensions was followed by measuring their optical absorbance as a function of time. By previously calculating the extinction cross section of particle doublets, it was demonstrated that for both core and core/shell particles the turbidity of the suspensions should increase on aggregation. Such an increase was in fact found in the systems in spite of the ever-present tendency of the particles to settle under gravity. The authors used the initial slope of the turbidity increment time plots as a measure of the ease of aggregation between particles. Thus, they found that the essential role played by pH on the charge generation on the two oxides and the shift of one pH unit between the isoelectric points of hematite and yttria manifest in two features: (i) the stability decreases on approaching the isoelectric point from either the acid or basic side and (ii) the maximum instability is found for hematite at pH 7 and for hematite/yttria at pH 8, that is, close to the isoelectric points of α-Fe_2O_3 and Y_2O_3, respectively. The role of added electrolyte is simply to yield the suspensions of either type more unstable. Using the surface free energy of the particles, the authors could estimate their Hamaker constants in water. From these and their zeta potentials, the DLVO theory of stability was used to quantitatively explain their results.

Key Words: **core/shell particles; hematite/ytrium oxide; turbidity; stability.**

INTRODUCTION

Currently, there exist a large variety of technological applications of composite colloidal particles consisting of a nucleus and a shell with different compositions. Like in many other fields of colloid science, special interest exists on such particles when they can be prepared with controlled shape and size (1–5). In any case, the aim is to take advantage of the properties of both the nucleus (e.g., size, shape, magnetic susceptibility) and the shell (e.g., surface electrical characteristics, adsorption properties) materials. In the case of the particular combination chosen for the current study, the nucleus (hematite) is a well-known solid that can be prepared as colloidal particles of defined geometry, monodisperse in size and shape, and covering a wide range of both particle diameters (from about 50 nm to several microns) and geometries (including spheres, spheroids, cubes, or needles) (6, 7). They can be thought of as supports for other materials that cannot be prepared with such a high versatility. One of them is yttrium oxide, Y_2O_3, which displays a number of applications as a catalyst or catalyst support (8) or as a component of ceramic matrices (9). In many of these applications, it is essential to have control on the size and shape of the particles. One possible way to do so is to coat particles with tailored geometry with a layer of zirconia. Furthermore, such particles may be considered as models for the investigation of the properties of core-shell materials, as control is possible on both their size and their shape through their modification in the hematite nucleus.

In the current work, the method first devised by Aiken and Matijević (4) has been used for synthesizing spherical colloidal particles formed by a hematite (α-Fe_2O_3) nucleus and an yttrium oxide (Y_2O_3) shell. The feasibility and reproducibility of the synthesis route was first demonstrated by Aiken and Matijević (4), and other authors have subsequently investigated their light-scattering properties (10), surface characteristics (11–13), and magnetism (14).

The current article focuses on another essential feature of the colloidal behavior of the particles, namely, the stability of their suspensions. Optical absorbance data are used as a probe of their aggregation kinetics, and a comparison is made between their stability and that of suspensions of the pure hematite nuclei. The results can be considered as an independent proof of the efficiency of α-Fe_2O_3 coating by yttrium oxide, mainly considering that the differences between their isoelectric points (*i.e.p.* or pH of zero zeta potential) should manifest themselves in clearly distinguishable aggregation-pH trends. Hence, the observed stability behaviors are correlated in both types of particles with their surface electrical charge through the classical DLVO theory (15). The current investigation intends to complete in some aspects our previous research with these colloids; thus, while in Quirantes *et al.* (10) we analyzed the light scattering of individual particles in a largely stable suspension, here we focus on

[1] To whom correspondence should be addressed. Current address: Departamento de Física Aplicada, Facultad de Ciencias, Universidad de Granada, 18071 Granada, Spain. Fax: +34 958-243214. E-mail: adelgado@ugr.es.

0021-9797/02 $35.00

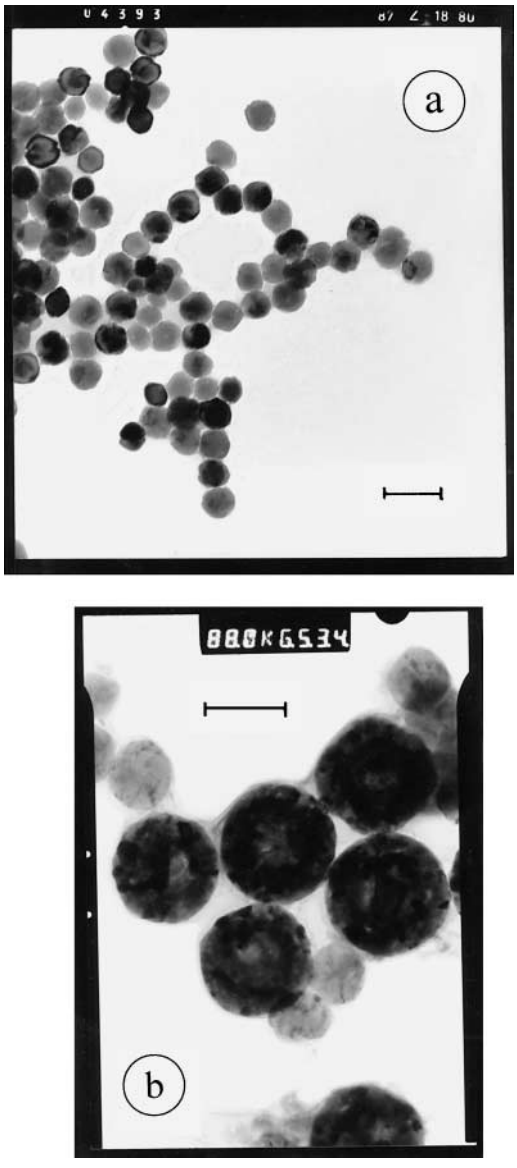

FIG. 1. Transmission electron micrographs of (a) hematite nuclei and (b) composite particles. Bar length: 100 nm.

the scattering of doublets of aggregated units and its application in the optical detection of such aggregation. On the other hand, our previous knowledge of the surface electrical characteristics of the coated particles (11, 12) is applied in this work to the explanation of the experimentally determined aggregation rates of the suspensions.

EXPERIMENTAL

Materials

The spherical hematite nuclei were obtained by homogeneous precipitation in a solution containing 0.018 M $FeCl_3$ (Merck, Germany) and 1 mM HCl (Carlo Erba, Italy). The solution was heated at 100°C for 24 h, following the procedure of Matijević and Scheiner (16). The suspension thus obtained was redispersed in Milli-Q water (Milli-Q Academic, Millipore, France) and repeatedly centrifuged at 15,000 rpm until the conductivity of the supernatant was below 2 μScm^{-1}. As shown in Fig. 1a, (obtained from a Zeiss EM902 Transmission Electron Microscope), spherical and reasonably monodisperse particles were obtained. Their average diameter was 60 ± 7 nm (see also Ref. 11).

The hematite/Y_2O_3 core/shell particles were prepared following Aiken and Matijević (4). The first step produced hematite particles covered by a layer of yttrium basic carbonate and consisted of heating during 9 h at 90°C suspensions containing 105 mg/l of hematite nuclei in 1.8 M urea (Panreac, Spain) +

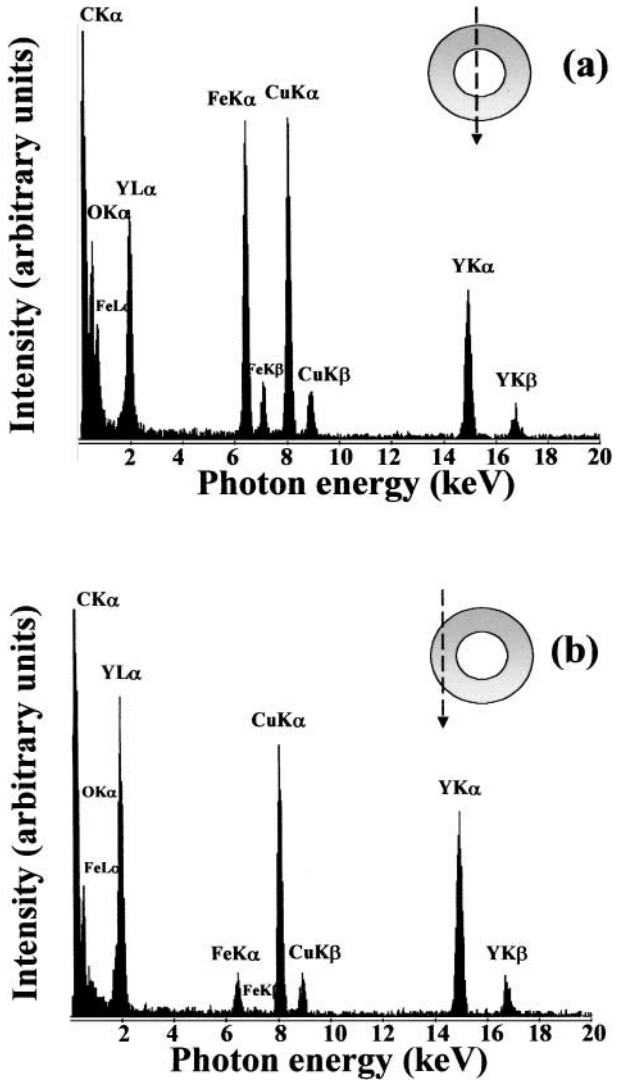

FIG. 2. Energy dispersive X-ray spectra of the nucleus (a) and the periphery (b) of the composite particles. The relative intensity of the characteristic X-ray lines indicated is plotted as a function of the photon energy. The dashed lines indicate the approximate regions of the particles were the analysis was performed.

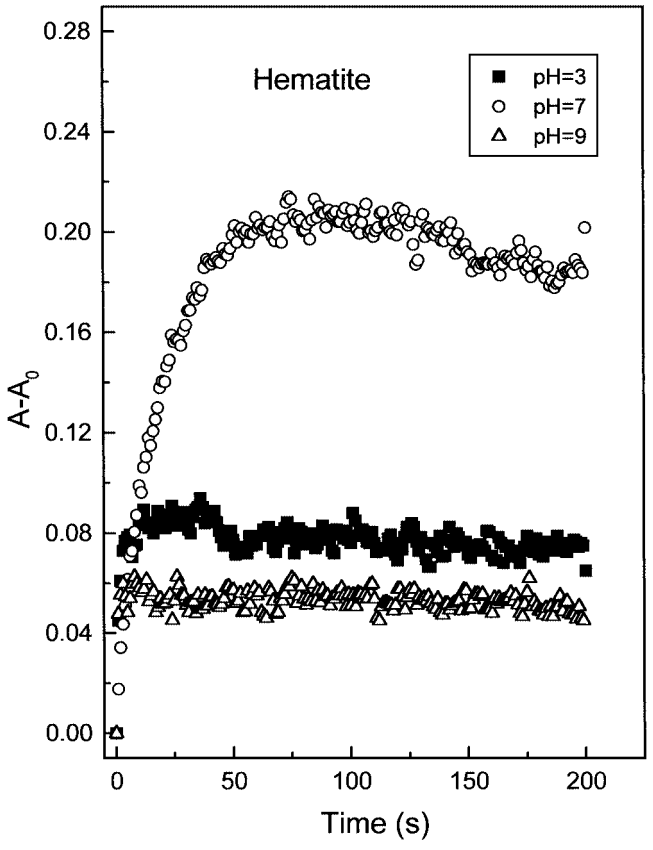

FIG. 3. Optical absorbance, A, referred to its initial value, A_0, as a function of time, for hematite suspensions of the pH values indicated. Ionic strength 10^{-3} M NaCl in all cases.

3 mM yttrium nitrate (Merck, Germany) solutions. The yttrium carbonate layer was subsequently converted to yttrium oxide by calcination of the mixed hematite/yttrium carbonate particles at 800°C for 3 h. The average diameter of the final particles was 150 ± 20 nm. Figure 1b (obtained from a Philips CM-20 High-Resolution Transmission Electron Microscope) shows the microstructure of the composite particles obtained; the presence of the nucleus (iron oxide) is distinguishable from the yttria shell. The EDX microanalysis probe attached to the microscope did, in fact, demonstrate that the chemical compositions of the nucleus and the periphery were clearly different. Figure 2 is an example of the results obtained. Apart from the presence of copper and carbon lines (coming from the carbon coating and the microscope grid), it can be observed that yttrium is clearly more abundant in the external part of the particles, whereas iron is in the nucleus, as expected.

METHODS

The stability of the suspensions was inferred from optical absorbance measurements as a function of time using a Milton–Roy Spectronic 601 (United States) UV-VIS spectrophotometer set at 600 nm. Absorbance data were recorded at 1-s intervals during 200 s. All suspensions had 2 g/l concentration of solids, and the effects of both pH (at constant ionic strength, 10^{-3} M NaCl) and ionic strength (at pH 6, the natural pH of the systems) were investigated.

RESULTS AND DISCUSSION

Experimental Stability Determinations

Figures 3 and 4 show examples of the absorbance–time trends of the hematite and composite particles, respectively. The quantity plotted is the absorbance increment, that is, the difference between the absorbance, A, at any time and the initial absorbance, A_0. Although in most cases the long-time behavior corresponds to a decrease of absorbance due to the settling of the particles, the initial slopes of the curves can be either positive or negative and, in fact, yield the most significant information about particle–particle aggregation.

The initial increase in absorbance found in all of the examples of Figs. 3 and 4, in spite of the tendency of the particles to sediment out of the light beam, seems an indication of the fact that a doublet of particles has a larger extinction cross section, C_{ext}, than two individual units sufficiently far apart. The scattering of light by particle aggregates is a difficult problem, complicated by the fact that one of the colloidal systems investigated

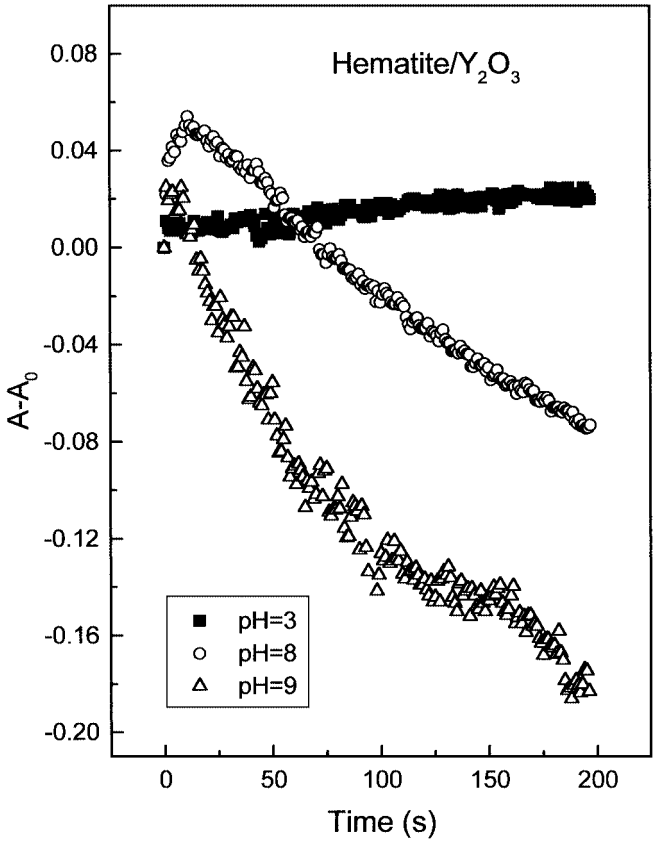

FIG. 4. Same as Fig. 3, but for hematite/Y_2O_3 core/shell particles.

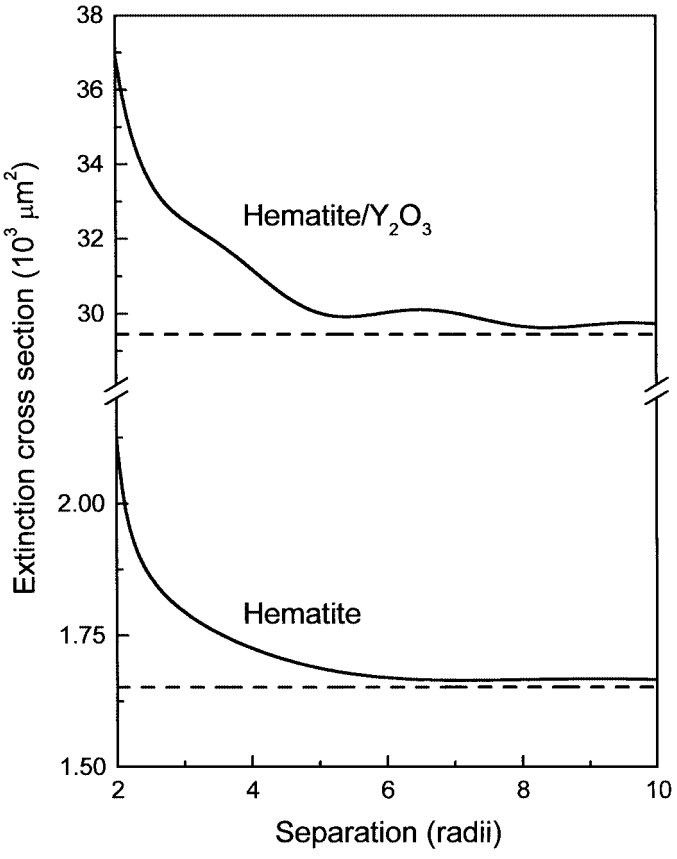

FIG. 5. Extinction cross sections of doublets of hematite cores and hematite/Y_2O_3 core/shell particles as a function of the center-to-center particle separation. The dashed lines indicate the infinite separation values.

consists of core-shell particles. However, there exist methods that permit a rigorous calculation of C_{ext}, particularly when aggregates of only two spheres are considered (17–19). This situation is most likely to occur during the initial stages of aggregation; hence, they can be useful in explaining the results of Figs. 3 and 4 for short aggregation times. The T-matrix (or EBCM) method, combined with the superposition formulation for radiative interactions between spheres (17, 18), has been used in the current work for the calculation of C_{ext} in bispherical particle systems. Thus, Fig. 5 shows how the extinction cross sections of both core and coated particles increase with decreasing separation. Note that when particles are in contact, C_{ext} increases by a factor of 1.29 (1.25) for bare (coated) particles as compared with the extinction coefficient of two individual spheres. As a consequence, the first stages of aggregation will be characterized by an increase in absorbance, as found experimentally (Figs. 3 and 4). It is important to point out that this is not a universal observation given that light-scattering interactions will depend on both particle size and composition. As an example, Fig. 6 shows that C_{ext} for two contacting spheres of the same compositions as our core and coated particles can be lower than the value corresponding to infinitely separated spheres for particle diameters roughly above 300 nm. Hence, care must be taken when interpreting absorbance data of interacting particles because the trend of variation of C_{ext} on close approach of the particles is not known.

The initial slopes of absorbance curves like those in Figs. 3 and 4 are plotted, as a function of pH, in Fig. 7 for both hematite and mixed particles. Note how the slopes for acid solutions are positive and increase with pH until reaching a maximum close to pH 7 for hematite and close to pH 8 for the mixed particles. A further increase in pH yields a significant decrease of the slope that even becomes negative in the case of the core/shell particles. This behavior can be understood qualitatively in terms of the values of the pH_{iep} of both kinds of particles (7): pH = 7.5 for hematite and pH = 8.5 for the mixed colloids. The absence of electrostatic double-layer repulsions between the particles for those pH values brings about a rapid aggregation, and hence a fast increase in absorbance, as a consequence of the abovementioned increase in scattering cross sections of doublets as compared with pairs of individual particles. The differences between the specific values of $d(A - A_0)/dt$ for both kinds of particles are related to the larger diameter of core/shell units, but with the general trends being essentially identical.

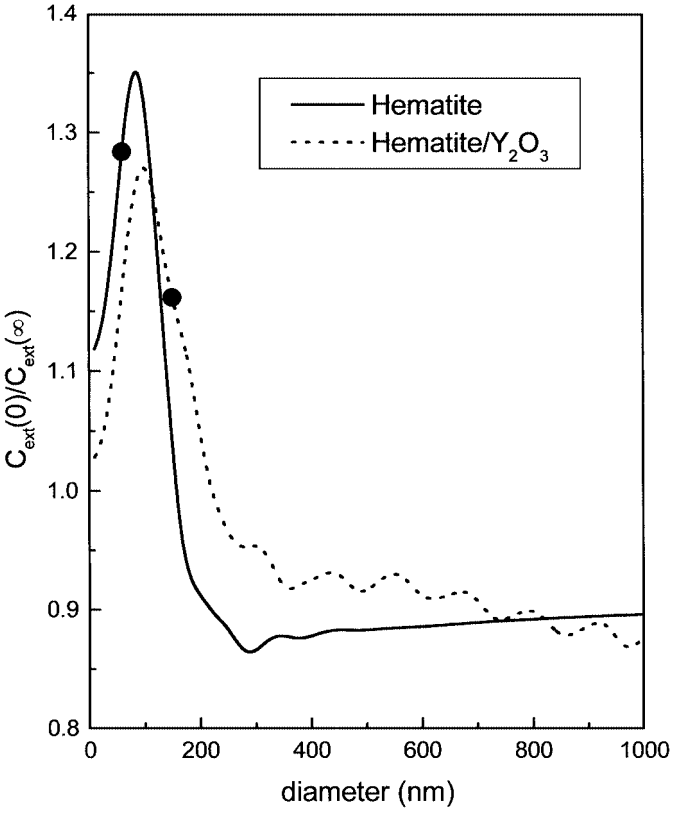

FIG. 6. Calculated ratio between the extinction cross section of two contacting spheres, C_{ext} (0), and two spheres at infinite separation, C_{ext} (∞), as a function of particle diameter. The composition of the spheres is assumed identical to that of hematite and hematite/Y_2O_3 particles. The circles indicate the location of the particles studied in this work.

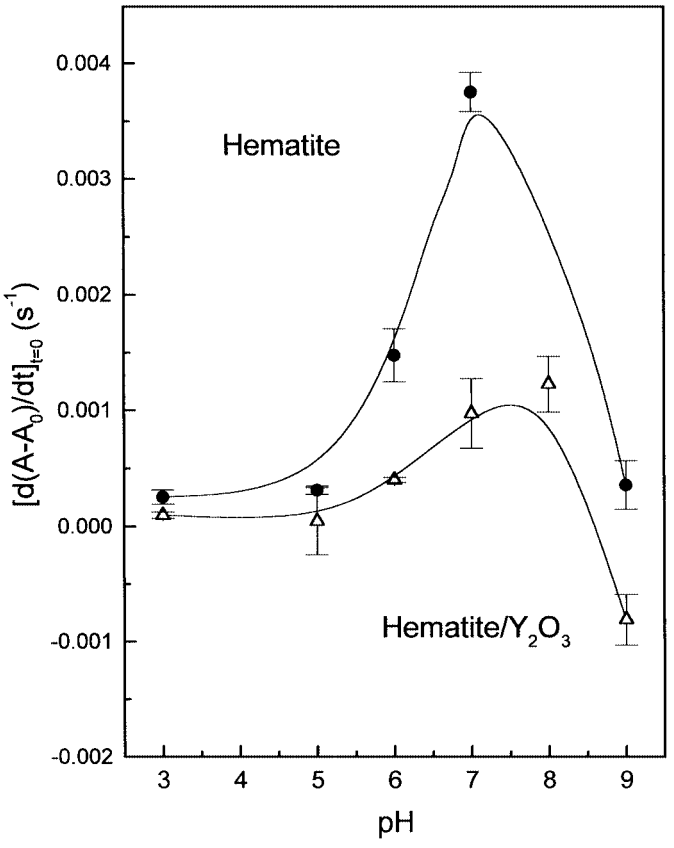

FIG. 7. Initial slopes of absorbance increments like those plotted in Figs. 2 and 3 as a function of pH for hematite nuclei and composite particles. The dispersion media were 10^{-3} M NaCl solutions in all cases. Error bars correspond to the 95% confidence interval of the slopes of the straight lines fitted to the low-time data.

The same applies to the effect of NaCl concentration on the initial absorbance slopes. Our data (not shown here for the sake of brevity) yield an increase of the slopes with ionic strength in a practically monotonous fashion for the two types of materials. The screening of electrical double-layer repulsions by increasing amounts of ionic species in the medium can account for the faster aggregation, that is, the faster increase in turbidity found for both hematite and core/shell particles as larger concentrations of NaCl are added to the supporting solution.

Potential Energy of Interaction between the Particles

The experimental data just described should now be compared with theoretical predictions based on the classical DLVO theory of the stability of colloids (15). The total potential energy of interaction is the sum of two contributions, namely, electrostatic double-layer repulsion, $V^{EL}(s)$, and Lifshitz–van der Waals attraction $V^{LW}(s)$. The following equation is used for the former:

$$V^{EL}(s) = 2\pi\varepsilon_r\varepsilon_0 a\zeta^2 \ln(1 + e^{-\kappa s}), \qquad [1]$$

where $\varepsilon_r\varepsilon_0$ is the dielectric permitivity of the solution, a is the particle radius, $s = r - 2a$ (with r being the center-to-center distance between the particles), and κ is the reciprocal double-layer thickness. In Eq. [1], the zeta potential, ζ, is used as our best estimation of the diffuse potential, ψ_d (potential at the beginning of the diffuse layer). This is a good approximation, provided the potential is not too high.

The Lifshitz–van der Waals attraction has been calculated according to the following expression (20):

$$V^{LW}(s) = -\frac{A}{6}\left[\frac{2a^2}{s(4a+s)} + \frac{2a^2}{(2a+s)^2} + \ln\frac{s(4a+s)}{(2a+s)^2}\right], \qquad [2]$$

where A is the Hamaker constant, depending on the type of particles and on the dispersion medium between them. Because A is not known for the systems that we are investigating, it was estimated from surface free energy determinations (9). Thus, we have the following expression (21):

$$A = 24\pi s_0^2\left(\sqrt{\gamma_S^{LW}} - \sqrt{\gamma_L^{LW}}\right)^2, \qquad [3]$$

where s_0 is the so-called equilibrium separation distance between the interfaces, and a good estimation of it yields $s_0 = 1.58 \pm 0.08$ Å (21), and γ_X^{LW} is the Lifshitz–van der Waals component of the surface free energy of the solid ($X \equiv S$) and the surface tension of the liquid ($X \equiv L$). Taking the latter to be water (addition of relatively small concentrations of electrolyte does not change the value γ_L^{LW} of as compared with that of pure water) $\gamma_L^{LW} = 21.8$ mJ/m^2 (22). The values for the solids have been evaluated from contact angle measurements as determined in Ref. 21. The details are given in Ref. 13. The resulting values are $A = 0.138\times\ 10^{-20}$ J (hematite core) and $A = 0.178 \times 10^{-20}$ J (core/shell particles). Table 1 summarizes all of the other data needed in the evaluation of $V(s) = V^{EL}(s) + V^{LW}(s)$.

TABLE 1
Quantities Required for the Calculation of $V^{EL}(s)$ and $V^{LW}(s)$ (Eqs. [1] to [3]) for the Systems under Study

Material	pH	[NaCl]M	ζ (mV)	κ (nm^{-1})
Hematite	6	10^{-2}	8	0.333
	6	5×10^{-3}	12	0.232
	6	10^{-3}	16	0.105
	6	5×10^{-4}	20	0.073
	3	10^{-3}	35	0.105
	5	10^{-3}	24	0.105
	7	10^{-3}	6	0.105
	9	10^{-3}	−18	0.105
Hematite/Y_2O_3	6	10^{-2}	26	0.333
	6	5×10^{-3}	33	0.232
	6	10^{-3}	45	0.105
	6	5×10^{-4}	48	0.073
	3	10^{-3}	60	0.105
	5	10^{-3}	55	0.105
	7	10^{-3}	27	0.105
	8	10^{-3}	1	0.105
	9	10^{-3}	−21	0.105

Using these data and Eqs. [1] to [3], the potential energy curves plotted in Figs. 8 and 9 are easily obtained. Note how the experimental data in Fig. 7 (as well as those mentioned above for the effect of NaCl concentration on stability) are explained in view of the relative tendencies of $V(s)$ when pH and ionic strength are changed. At pH 7 (hematite, Fig. 8a) and pH 8 (hematite/Y_2O_3, Fig. 9a), the potential energy yields an essentially attractive interaction at all distances, while the latter becomes repulsive for any distance above ~5 nm for any other pH value. The short-range attraction observed for shorter separations can take place only if the particles surpass the maxima found at such critical distances. The height of those maxima is larger, the greater the difference between the actual pH and the isoelectric point. Note also that the larger particle size of hematite/yttria composites yields higher maxima. In all other aspects, the general trends of $V(s)$ curves with pH are similar for both types of particles. Similar conclusions can be reached on analyzing the effect of NaCl concentration (Figs. 8b and 9b): for concentrations $\geq 10^{-3}$ M NaCl, the electrical double-layer repulsion is nearly negligible, thus yielding very unstable systems and, correspondingly, large slopes of the initial absorbance increase.

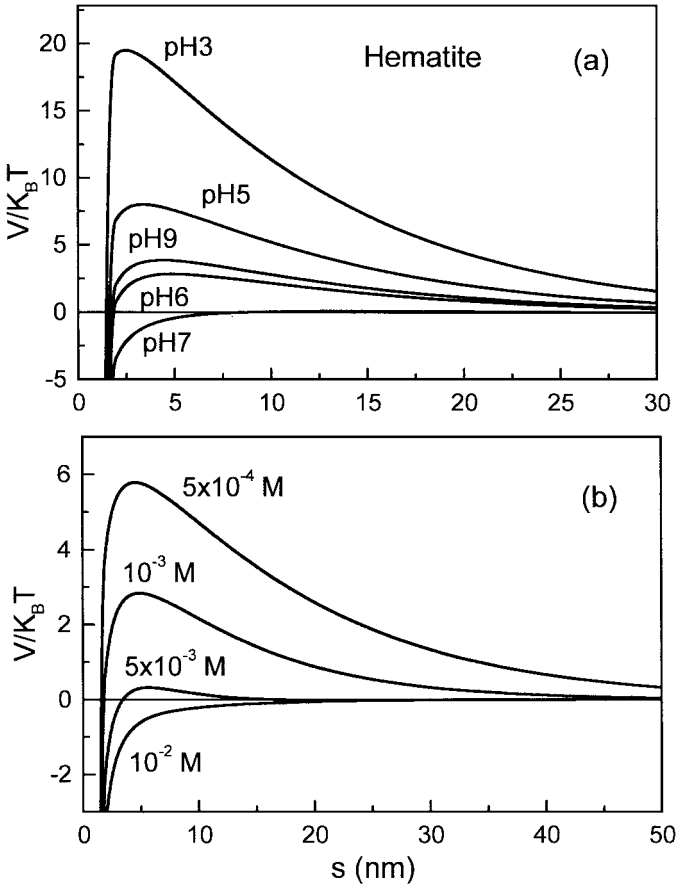

FIG. 8. Potential energy $V(=V^{EL}+V^{LW})$ of interaction between hematite particles as a function of surface-to-surface distance (s). (a) Effect of pH in 10^{-3} M NaCl solutions. (b) Effect of NaCl molar concentration at pH 6.

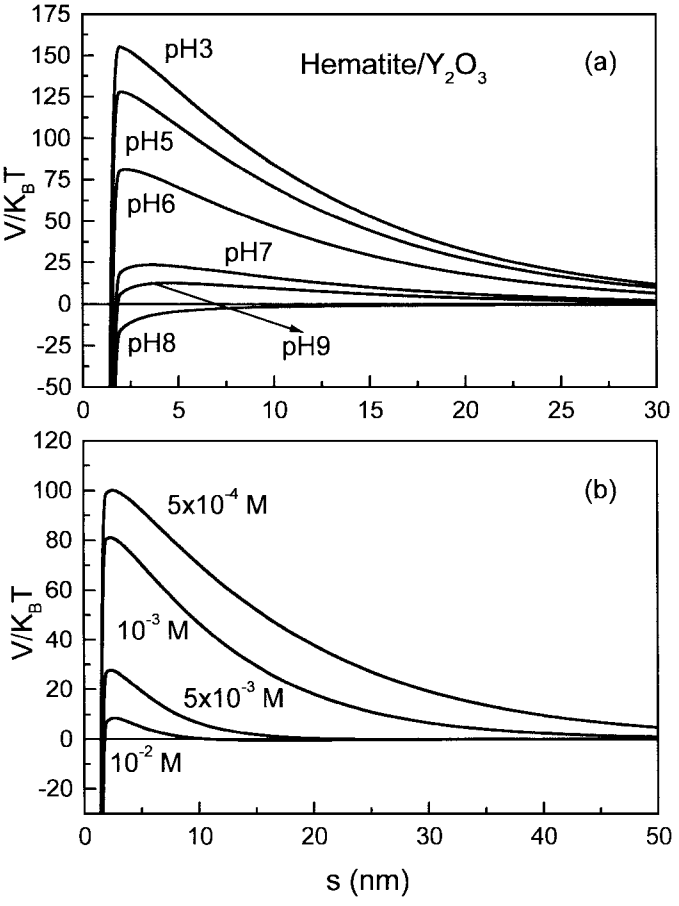

FIG. 9. Same as Fig. 7, but for hematite/Y_2O_3 core/shell particles.

CONCLUSION

In this work, we have shown that spherical hematite particles can be efficiently covered by a layer of yttrium oxide and that the colloidal stability, a fundamental property of the systems, is most sensitive to the surface modification involved. Using data on the time rate of turbidity changes for different pH values and ionic strengths, it is shown that the composite particles behave as if formed entirely by yttria, particularly concerning the large instability exhibited by the particles in the vicinity of the isoelectric point of yttrium oxide. The classical DLVO theory is used to explain the results obtained, after estimation of the Hamaker constants of both bare and coated nuclei, using surface free energy determinations of the solids.

ACKNOWLEDGMENTS

Financial support from MCYT, Spain (Project MAT2001-3801) and INTAS (Project 99-00510) is gratefully acknowledged.

REFERENCES

1. Gherardi, P., and Matijević, E., *J. Colloid Interface Sci.* **109,** 57 (1986).
2. Kratohvil, S., and Matijević, E., *Adv. Ceramic Mater.* **118,** 506 (1987).

3. Magville, F. C., Partch, R. E., and Matijević, E., *J. Colloid Interface Sci.* **120,** 135 (1987).
4. Aiken, B., and Matijević, E., *J. Colloid Interface Sci.* **126,** 645 (1988).
5. Garg, A., and Matijević, E., *Langmuir* **4,** 38 (1988).
6. Matijević, E., *Annu. Rev. Mater. Sci.* **15,** 483 (1985).
7. Matijević, E., and Sapieszko, R. S., *in* "Fine Particles: Synthesis, Characterization, and Mechanisms of Growth" (T. Sugimoto, Ed.), pp. 18–22. Marcel Dekker, New York, 2000.
8. Márquez-Álvarez, C., Fierro, J. L. G., Guerrero-Ruiz, A., and Rodríguez-Ramos, I., *J. Colloid Interface Sci.* **159,** 454 (1993).
9. Garg, A., and Matijević, E., *J. Colloid Interface Sci.* **126,** 243 (1988).
10. Quirantes, A., Plaza, R. C., and Delgado, A. V., *J. Colloid Interface Sci.* **189,** 236 (1997).
11. Plaza, R. C., Durán, J. D. G., Quirantes, A., Ariza, M. J., and Delgado, A. V., *J. Colloid Interface Sci.* **194,** 398 (1997).
12. Plaza, R. C., González-Caballero, F., and Delgado, A. V., *Colloid & Polymer Sci.* **279,** 1206 (2001).
13. Plaza, R. C., Zurita, L., Durán, J. D. G., González-Caballero, F., and Delgado, A. V., *Langmuir* **14,** 6850 (1998).
14. Plaza, R. C., Gómez-Lopera, S. A., and Delgado, A. V., *J. Colloid Interface Sci.* **240,** 48 (2001).
15. Hunter, R. J., "Foundations of Colloid Science," Clarendon, Oxford, UK, 1987.
16. Matijević, E., and Scheiner, P., *J. Colloid Interface Sci.* **63,** 509 (1978).
17. Mackowski, D. W., *Proc. R. Soc. London A* **433,** 599 (1991).
18. Mishchenko, M. I., Mackowski, D. W., and Travis, L. D., "Light Scattering by Nonspherical Particles," Academic Press, San Diego, 2000.
19. Quirantes, A., Arroyo, F., and Quirantes-Ros, J., *J. Colloid Interface Sci.* **240,** 78 (2001).
20. Gregory, J., *J. Colloid Interface Sci.* **22,** 342 (1966).
21. van Oss, C. J., "Interfacial Forces in Aqueous Media," Marcel Dekker, New York, 1994.
22. van Oss, C. J., and Good, C. J., *J. Macromol. Sci. Chem. A* **26,** 1183 (1989).